Analysis of traffic jerk effect in a new lattice model with density-dependent passing

Muskan Verma and Sapna Sharma

Abstract In real traffic dynamics, non-motor vehicles often undergo sudden acceleration changes while passing, leading to traffic congestion on roads. Thus, a lattice model is modified to examine the impact of traffic jerk, taking into account the density-dependent passing behavior. The linear stability analysis is performed. It is found that the stability region reduces considerably with an increasing traffic jerk coefficient. By the reduction perturbation method, the kink-antikink soliton wave solution of the mKdV equation is attained, which describes the propagation of the density wave near the critical point. The theoretical results are validated by numerical simulation.
Keywords: Traffic jerk, Passing, Lattice model, Traffic flow

1 Introduction

Over the decades, traffic jams have worsened due to the rapid growth of population, rapid urbanization, increasing number of vehicles, the surge in e-commerce sections, inadequate infrastructure, and a lot more. This may result in numerous issues like environmental pollution, safety hazards, vehicular queuing, etc. Thus, to comprehend and minimize traffic jam/congestion, various theories, and mathematical models [1, 2, 3, 4, 5, 6, 7, 8, 9, 10, 11, 12, 13, 14, 15] are proposed to optimize the traffic flow.

Under normal traffic conditions with uniform flow, vehicles do not need to pass/overtake. However, overtaking becomes essential as the number of vehicles increases but within capacity. This indicates that passing increases as vehicular den-

Muskan Verma
School of Mathematics, Thapar Institute of Engineering and Technology, Patiala-147004, India, e-mail: muskan0818@gmail.com

Sapna Sharma
School of Mathematics, Thapar Institute of Engineering and Technology, Patiala-147004, India e-mail: sapna.sharma@thapar.edu

K. R. Rao et al. (eds.), *Traffic and Granular Flow '22* , Lecture Notes in Civil Engineering 443, https://doi.org/10.1007/978-981-99-7976-9_45

sity increases. However, as the density increases continually, traffic jams occur, and if overtaking occurs, it contributes to chaos and further congestion on roads. So, the increasing density leads to congestion/ jams on the road. Thus, a new lattice model was proposed incorporating the density-dependent passing [15]. Furthermore, the unanticipated acceleration changes of non-motor vehicles, called traffic jerks, can lead to traffic congestion and even cause traffic accidents. Keeping this view in mind, Ge et al. [16] proposed a model considering the traffic jerk parameter and concluded that the uneven motion of non-motor vehicles would increase traffic jams. Redhu and Siwach [17] extended the lattice model taking into account the impact of traffic jerk. It is observed that traffic jerk parameter plays a significant role in stabilizing the traffic flow. While passing, it is often seen that the vehicles undergo sudden acceleration changes, which may increase traffic congestion. A lattice model is extended in Section 2, considering density-dependent passing to examine the effect of traffic jerk in such scenarios.

The following sections of the paper are outlined as Section 3 presents the linear stability analysis. Following that, a reduction perturbation method is conducted to analyze the traffic flow behavior. The computation of kink-antikink wave solution is described near the critical point (ρ_c, a_c) in Section 4. In Section 5, numerical simulations are performed. Lastly, Section 6 provides the conclusion of the paper.

2 Proposed Model

In the proposed work, we are incorporating the impact of traffic jerk, taking into account the density-dependent passing [15]. the continuity equation for the model is conserved as there are no sinks or sources and is given as

$$\rho_j(t+\tau) - \rho_j(t) + \tau\rho_0[\rho_j(t)v_j(t) - \rho_{j-1}(t)v_{j-1}(t)] = 0. \tag{1}$$

Here, ρ_0 is average density, $\tau = \frac{1}{a}$ is the delay time, the subscript j denotes the site j on a one-dimensional lattice. Also, $\rho_j(t)$ and $v_j(t)$ represent the vehicular density and average speed at site j, respectively.

While passing, it is often seen that the vehicles undergo sudden acceleration changes, which may increase traffic congestion. Therefore, the evolution equation is modified to investigate the traffic jerk effect with the consideration of density-dependent passing and is given as:

$$\begin{aligned}\rho_j(t+\tau)v_j(t+\tau) = \rho_0 V(\rho_{j+1}(t)) + \gamma(\rho_{j+1}(t))[\rho_0 V(\rho_{j+1}(t)) - \rho_0 V(\rho_{j+2}(t))] \\ -\lambda[\rho_j(t)v_j(t) - \rho_j(t-\tau)v_j(t-\tau)]\end{aligned} \tag{2}$$

where $V(.)$ is optimal velocity function, $\gamma(\rho_{j+1}(t))$ represents the amount of traffic passing on-site $j+1$ at time t considered as in Ref. [15].

The density equation is formed using Eqs. (1) and (2) as

$$\rho_j(t+2\tau) - \rho_j(t+\tau) + \tau\rho_0^2[V(\rho_{j+1}(t)) - V(\rho_j(t))] - \tau\rho_0^2[\gamma(\rho_{j+1}(t))V(\rho_{j+2}(t) - (\gamma(\rho_{j+1}(t)) + \gamma(\rho_j(t)))V(\rho_{j+1}(t)) + \gamma(\rho_j(t))V(\rho_j(t))] - \lambda(-\rho_j(t+\tau) + 2\rho_j(t) - \rho_j(t-\tau)) = 0 \quad (3)$$

When $\lambda = 0$, the equation is analogous as given in Ref. [15].

3 Linear stability analysis

To examine the influence of traffic jerk coefficient on traffic flow with density-dependent passing, the stability analysis is conducted. At steady-state, the vehicular density and average speed are taken as:

$$\rho_j(t) = \rho_0, v_j = V(\rho_0) \quad (4)$$

Performing the analysis [15], neutral stability condition is obtained as

$$\tau = -\frac{1 - 2\gamma(\rho_0)}{(3 + 2\lambda)\rho_0^2 V'(\rho_0)}. \quad (5)$$

The instability in traffic flow is observed when

$$\tau > -\frac{1 - 2\gamma(\rho_0)}{(3 + 2\lambda)\rho_0^2 V'(\rho_0)} \quad (6)$$

Eq. (5) shows that the traffic jerk coefficient significantly stabilizes the traffic flow

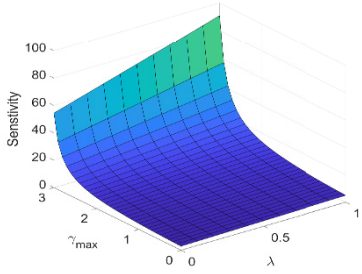

Fig. 1 Neutral stability curves when $\theta = 4$, $E = 10$

for a one-dimensional traffic system. Also, stability condition obtained is analogous to the case discussed in [15] when $\lambda = 0$. Fig. 1 illustrates the neutral stability curves in the parameter space $(\lambda, \gamma_{max}, a)$. It is evident from the figure that the instability of traffic flow increases as the value of λ increases resulting in increased traffic jams.

Also, when γ_{max} increases, the delay time decreases significantly, indicating that traffic flow stability is suppressed significantly.

4 Reduction Perturbation Method

To understand the traffic dynamics near the critical point (ρ_c, a_c) on coarse-grained scales, the slow variables X and T are considered for a small positive parameter ϵ, where $(0 < \epsilon \leq 1)$ as follows:

$$X = \epsilon(j + bt), T = \epsilon^3 t \tag{7}$$

where b is the constant to be computed. The density ρ_j is taken as:

$$\rho_j(t) = \rho_c + \epsilon R(X, T) \tag{8}$$

g_1	$\frac{1-13\gamma(\rho_c)-14\gamma(\rho_c)^2+2\lambda^2(1+6\gamma(\rho_c))-36\gamma(\rho_c)\lambda+6\lambda}{3(3+2\lambda)^2}(-\rho_c^2 V'(\rho_c))$
g_2	$\frac{\rho_c^2 V'''(\rho_c)}{6}$
g_3	$\frac{(1-2\gamma(\rho_c))}{2}(-\rho_c^2 V'(\rho_c))$
g_4	$\frac{-9+52\lambda+54\lambda^2+12\lambda^3+4\gamma^3(99+58\lambda)+6\gamma^2(9+158\lambda+48\lambda^2-32\lambda^3+6\gamma(9-52\lambda-6\lambda^2+20\lambda^3))}{12(3+2\lambda)^3}(-\rho_c^2 V'(\rho_c))$
g_5	$\frac{1-4\gamma(\rho_c)}{12}(-\rho_c^2 V'''(\rho_c)) - \frac{\rho_c^2 V'(\rho_c)\gamma''(\rho_c)}{6}$
g_6	$-\frac{\gamma\rho_c^2 V'''}{2}$

Table 1

Using Taylor's expansion, Eq.(9) is obtained as in Ref. [15]:

$$\epsilon^4(\partial_T R - g_1\partial_X^3 R + g_2\partial_X R^3) + \epsilon^5(g_3\partial_X^2 R + g_4\partial_X^4 R + g_5\partial_X^2 R^3 + g_6 R^2\partial_X^2 R) = 0 \tag{9}$$

where the coefficients $g_i, (i = 1, 2, ..., 6)$ are given in Table 1. The following transformations are considered to derive a standard mKdV equation:

$$T' = g_1 T, R = \sqrt{\frac{g_1}{g_2}} R' \tag{10}$$

where we assumed $g_1 > 0$, which gives the existence condition as

$$1 - 13\gamma(\rho_c) - 14\gamma(\rho_c)^2 + 2\lambda^2(1 + 6\gamma(\rho_c)) - 36\lambda\gamma(\rho_c) + 6\lambda > 0. \tag{11}$$

The regularized equation is given by

$$\partial_{T'} R' - \partial_X^3 R' + \partial_X R'^3 + \epsilon M[R'] = 0, \tag{12}$$

where $M[R'] = \frac{1}{g_1}[g_3\partial_X^2 R' + g_4\partial_X^4 R' + \frac{g_1 g_5}{g_2}\partial_X^2 R'^3 - 3\gamma(\rho_c)R'^2\partial_X^2 R']$. By ignoring the $O(\epsilon)$ correction term, equation (12) reduces to the standard mKdV equation. The solution obtained is kink-antikink and is given as:

$$\rho_j = \rho_c + \epsilon\sqrt{\frac{g_1 c}{g_2}}\tanh\left(\sqrt{\frac{c}{2}}(X - cg_1 T)\right). \tag{13}$$

with $\epsilon^2 = \frac{a_c}{a} - 1$ and the amplitude A of the solution is $A = \sqrt{\frac{g_1}{g_2}\epsilon^2 c}$. The above solution is valid if condition (11) is satisfied. Therefore, the existing condition is given by

$$0 \le \gamma_{max} < f(E, \theta, \lambda) \tag{14}$$

where

$$f(E,\theta,\lambda) = \frac{1}{28}\left(\frac{1 + E(\frac{\rho_c}{\rho_m})^\theta}{\rho_c(1 - \frac{\rho_c}{\rho_m})}\right)\left(-13 - 36\lambda + 12\lambda^2 + \sqrt{K}\right). \tag{15}$$

where

$$K = 225 + 1272\lambda + 1096\lambda^2 - 864\lambda^3 + 144\lambda^4$$

Thus, two cases arise:

Case 1: When $0 \le \gamma_{max} < f(E, \theta, \lambda)$, the mKdV equation exists, and in a specific case, when $\lambda = 0$, the existence condition for the kink solution agrees with the one obtained in [15]. Moreover, the kink-antikink solution of the mKdV equation represents the coexisting curves which include both freely moving and jammed phases described by $\rho_j = \rho_c \pm A$ in phase space (ρ_c, a_c).

Case 2: When $\gamma \ge f(E, \theta, \lambda)$, the mKdV equation does not exist.

From reduction perturbation method, the obtained coexisting curves divide the phase plane into three regions: stable, metastable, and unstable regions, as shown in Fig. 2 (a). The apex of neutral stability and coexisting curves increases corresponding to higher values of λ, indicating unstable traffic flow. Fig. 2 (b) illustrates the phase

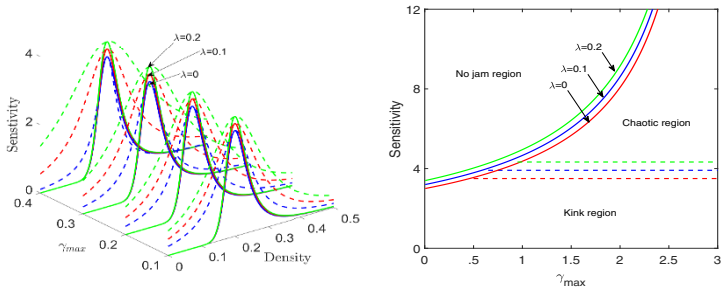

(a) (b)

Fig. 2 **(a)** Phase diagram in $(\rho_0, \gamma_{max}, a)$ **(b)** Phase plot in parameter space (γ_{max}, a) when $\theta = 4$, $E = 10$

plot in space (γ_{max}, a) for different values of λ, where $\theta = 4$, $\rho_c = 0.2$. The boundary line that separates kink region from the chaotic region is given by equation $a = \frac{3+2\lambda}{1-2\gamma(\rho_c)}$. The transitions appears from no jam region to kink region with decreasing sensitivity, via chaotic jam region. As the value of λ increases, the free flow region decreases while the chaotic region enhances which results in a traffic jam. Also, with the increase in traffic jerk coefficient λ, kink jam region increases.

5 Numerical Simulation

To validate the analytical results obtained from the stability analysis performed in the above sections, numerical simulations are conducted under periodic boundary conditions. The following initial condition is taken:

$$\rho_j(0) = \begin{cases} \rho_0 - A, & \text{for } 0 \le j < \frac{L}{2} \\ \rho_0 + A, & \text{for } \frac{L}{2} \le j < L \end{cases}, \rho_j(1) = \begin{cases} \rho_0 - A, & \text{for } 0 \le j < \frac{L}{2} - m \\ \rho_0 + A, & \text{for } \frac{L}{2} - m \le j < L - m \end{cases}$$

where the initial disturbance is taken as $A = 0.005$, m is a positive integer, system size $L = 100$, the parameter $\rho_0 = \rho_c = 0.2$, $\rho_m = 1$.

The discussion of results is given as follows:

Case 1: $\gamma_{max} < f(E, \theta, \lambda)$

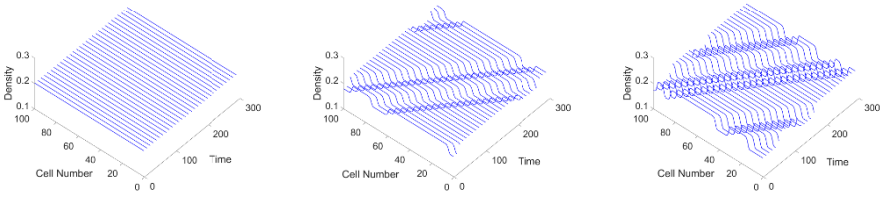

(a) (b) (c)

Fig. 3 Spatiotemporal evolutions of density at time $t = 20200$s when $a = 3.5$, $\theta = 4$, $E = 10$, $\gamma_{max} = 0.4$ for **(a)** $\lambda = 0$, **(b)** $\lambda = 0.1$, **(c)** $\lambda = 0.2$

To study the impact of λ on traffic flow, particular values of $\theta = 4$, $E = 10$ and $a = 3.5$ are considered when $\gamma_{max} = 0.4$. Fig. 3 represents the spatiotemporal evolutions of the density for $\lambda = 0$, 0.1, and 0.2. The uniform flow is observed for $\lambda = 0$. As λ increases, the amplitude of density waves also increases, indicating the kink antikink soliton waves. With an increase in traffic jerk coefficient λ, there is the transition from the free flow to a kink jam region, which leads to a decrease in the stability of traffic flow. Fig. 5 (a) represents the density profile at $t = 20200$s corresponding to Fig. 3. Thus, the increase in λ will make the traffic flow more unstable.

Case 2: $\gamma_{max} \geq f(E, \theta, \lambda)$

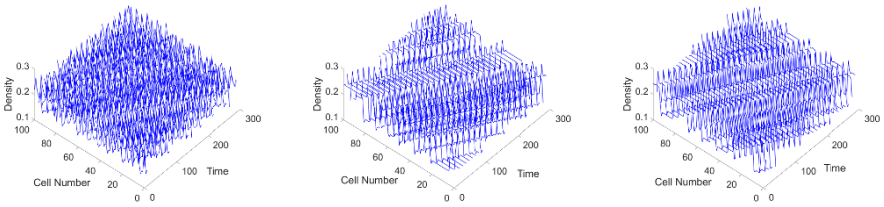

Fig. 4 Spatiotemporal evolutions of density at time $t = 20200$s when $a = 3.5$, $\theta = 4$, $E = 10$, $\gamma_{max} = 2.5$ when **(a)** $\lambda = 0$, **(b)** $\lambda = 0.1$, **(c)** $\lambda = 0.2$

Fig. 4 shows the spatiotemporal evolution of the density for $\lambda = 0$, 0.1 and 0.2, where parameters $\theta = 4$, and $a = 3.5$, $E = 10$, $\gamma_{max} = 2.5$. The density profiles at $t = 20200$s are shown in Fig. 5 (b). The density waves appear chaotic for $\lambda = 0$. Whereas for $\lambda = 0.1$, and 0.2, the amplitude of density waves decreases. Therefore, as the value of λ increases, the transition takes place from chaotic to kink jam region in an unstable region.

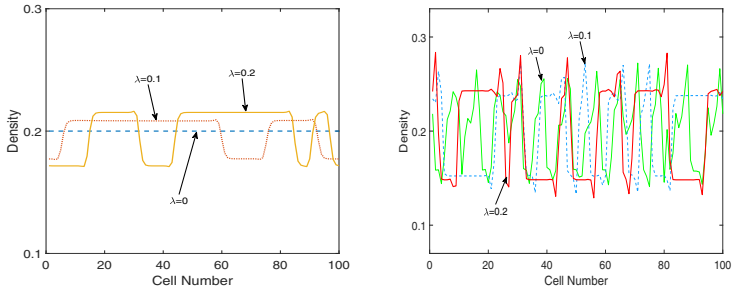

Fig. 5 Density profile at $t = 20200$s for $\theta = 4$, $E = 10$ **(a)** $a = 3.35$ when $\gamma_{max} = 0.4$, **(b)** $a = 3.5$ when $\gamma_{max} = 2.5$

6 Conclusion

We propose a modified lattice model to examine the impact of traffic jerk on traffic dynamics, taking into account density-dependent passing. The traffic behavior is analyzed theoretically through both linear and non-linear stability analyses. The neutral stability curves are derived, indicating that an increased traffic jerk coefficient results in increasing the unstable region, leading to traffic congestion. To describe

the propagation of density waves near the critical point, the modified Korteweg-de Vries (mKdV) equation is derived. Also, the existing condition is obtained for the kink-antikink soliton wave solution of the mKdV equation. Phase plots are discussed for different passing values. The transition takes place from the no-jam region to kink region for small passing values. When passing exceeds the critical value, a chaotic jam appears. Moreover, there is a transition from chaotic to kink jam region. Furthermore, increasing traffic jerk coefficient leads to an increase in the kink jam region. To validate the analytical findings, numerical simulations are conducted. It is found that numerical simulation aligns with the analytical results.

Acknowledgments

This work is supported by SERB-POWER SPG/2021/000591 funded by Science and Engineering Research Board (SERB), and authors are grateful to DST-FIST for the grant SR/FST/MS-1/2017/13 to support this research work.

References

1. H. Ge, S. Dai, L. Dong, Y. Xue, Physical Review E **70**(6), 066134 (2004)
2. P. Liao, T.Q. Tang, T. Wang, J. Zhang, Physica A: Statistical Mechanics and its Applications **525**, 108 (2019)
3. P. Berg, A. Mason, A. Woods, Physical Review E **61**(2), 1056 (2000)
4. C.F. Daganzo, Transportation Research Part B: Methodological **29**(4), 277 (1995)
5. A. Aw, M. Rascle, SIAM journal on applied mathematics **60**(3), 916 (2000)
6. R. Jiang, Q.S. Wu, Z.J. Zhu, Transportation Research Part B: Methodological **36**(5), 405 (2002)
7. A.K. Gupta, V. Katiyar, Transportmetrica **3**(1), 73 (2007)
8. A.K. Gupta, P. Redhu, Nonlinear Dynamics **76**(2), 1001 (2014)
9. T. Nagatani, Physica A: Statistical Mechanics and its Applications **264**(3-4), 581 (1999)
10. T. Nagatani, Physica A: Statistical Mechanics and its Applications **261**(3-4), 599 (1998)
11. T. Nagatani, Physical Review E **60**(2), 1535 (1999)
12. D. Kaur, S. Sharma, The European Physical Journal B **93**(3), 1 (2020)
13. P. Redhu, A.K. Gupta, Physica A: Statistical Mechanics And Its Applications **421**, 249 (2015)
14. S. Sharma, Nonlinear Dynamics **86**(3), 2093 (2016)
15. M. Verma, S. Sharma, Chaos, Solitons & Fractals **162**, 112435 (2022)
16. H.X. Ge, P.j. Zheng, W. Wang, R.J. Cheng, Physica A: Statistical Mechanics and its Applications **433**, 274 (2015)
17. P. Redhu, V. Siwach, Physica A: Statistical Mechanics and its Applications **492**, 1473 (2018)